공학석사 학위논문

Organic-Inorganic Composite Functional Separator to Reduce Shuttle Effect in Lithium Sulfur Battery

리튬 황-전지에서의 폴리설파이드의 셔틀 효과를 막는 기능성 분리막

2020년 2월

서울대학교 대학원

융합과학부 나노융합전공

조 진 일

Abstract

Organic-Inorganic Composite Functional Separator to Reduce Shuttle Effect in Lithium Sulfur Battery

Jinil Cho

Program in Nanoscience and Technology

The Graduate School of

Seoul National University

Lithium ion batteries (LIBs) have been used in portable electronic devices due to high energy density, rechargeable characteristics, and tiny memory effect. However, advanced portable electronic device, electric vehicles (EVs), and large scale energy storage system (ESS) require high specific capacity (energy density), light weight, and low cost LIBs.

The elemental sulfur is one of the most abundant materials on earth and has a

high theoretical capacity. However, there are some problems. The first problem is the dissolution of the polysulfide. The intermediate lithium polysulfides which was formed during the charge and discharge process are soluble in the typical organic electrolytes for LIBs. This leads to continuous cathode active material consumption, eventually the capacity is faded during cycle. The second problem is the safety and stability of the lithium metal used as the anode. Lithium metal surface control is a necessary step not only for the stability of Li metal anode, but also for a high capacity with a high coulombic efficiency(C.E).

In this study, we developed poly(vinylidene fluoride-co-hexafluoropropene) (PVdF-HFP) coated anodic aluminum oxide (PAAO) separator to blocking polysulfide shuttle effect and to control lithium metal interface. PAAO was prepared by coating PVdF-HFP solution on anodic aluminum oxide (AAO). AAO provides mechanically, chemically, and thermally stability. The vertical aligned pores of AAO are filled with PVdF-HFP which has been used as gel polymer electrolyte, offer high lithium ion conductivity with conventional electrolyte. PVdF-HFP selectively passes lithium ions and effectively blocks dissolution of the polysulfide into the anode region. Consequently, the proposed system conserved high specific capacity with high C.E. during the cycle. Prepared PAAO showed high specific capacity (～850 mAh g^{-1}, 0.2C), high C.E. (>98%), and long cycle life (>100 cycles, 0.5C). The suggested PAAO separator effectively block the polysulfide shuttle effect and improve the poor cyclability of the lithium-sulfur system. It suggests that this novel poreless separator can be a possible candidate of the powerful separator for lithium

sulfur batteries.

Keywords: lithium-sulfur batteries, lithium metal, polymer electrolyte, anodic aluminum oxide, next generation batteries

Student Number: 2018-21383

Table of Contents

List of Figures

Figure 7. Voltage profile of lithium sulfur cell with each separator at 0.5C. (a) first cycle, (b) 100th cycle

Figure 8. The voltage profile of Li symmetric cell cycled galvanostatically at 1 mA cm^{-2} for 500 cycles.

Figure 9. Optical Image of dissolution and diffusion of poly sulfide during the charge-discharge process.

Chapter 1. Introduction

1.1 Lithium sulfur batteries

Since the invention of lithium-ion batteries (LIBs) in the 1970s, they have been mainstays in determining the performance of electronic devices. In recognition of this merit, John B. Goodenough, M. Stanley Whittingham, and Akira Yoshino have been awarded the Nobel Prize in Chemistry in 2019, especially for the development of LIBs. In their early stages, LIBs were used in consumer electronics, especially mobile devices.[1]–[3] However, LIBs are now used in a wide range of applications, from mobile devices to large-scale energy storage such as electric vehicles and energy storage systems.[3]–[5] During such expansion in the breadth of applications, there has been a steady increase in the demand for higher energy density from these batteries. Conventional intercalation electrode materials such as lithium transition metal oxides and graphite are insufficient to meet these requirements because intercalation materials and their associated technologies have already achieved state-of-the-art limits. Ni-rich Li–Co–Ni–Al and Mn oxide, which is one of the highest-capacity intercalation materials, show specific capacities of approximately 200 mAh g^{-1}[6],[7], which is not adequate in terms of full cell capacity because this capacity represents

the series combination of cathode and anode capacities. Therefore, new types of cathodic materials have been studied. Representative materials for such applications include sulfur, which enables the conversion reaction; sulfur has a high theoretical specific capacity of 1675 mAh g^{-1}, which is eight times that of the Ni-rich ternary transition metal oxide. Sulfur is produced as a by-product in the petrochemical industry; however, it is used only to manufacture sulfuric acid, as a rubber additive, and as a fertilizer, thus abandoning a large quantity available in nature. This means that the supply could be stable and the price lower than conventional active materials.[8]

To utilize this high specific capacity of sulfur, anodic materials must have a reasonably high specific capacity. Li metal is the most suitable anode for using sulfur owing to its high theoretical capacity and low potential. Thus, lithium sulfur batteries (LSBs), which have a sulfur cathode and Li metal anode, were suggested.[9]–[11]

Despite their high specific capacities, LSBs have not yet been commercialized because of critical issues during their cycling. The most serious problem of an LSBs is sustained capacity fading by the "shuttle effect" of the lithium polysulfide species.[12] In the LSBs, the lithium polysulfide species is generated during discharge, and the mole ratio of Li to S varies depending on the depth of discharge. Lithium polysulfide species, especially high-sulfur-content lithium polysulfide, is highly

soluble in the electrolyte; the molecules are easily dissolved in the electrolyte and move to the anode region.[13] This lithium polysulfide can then be electrolyzed to Li_2S and Li_2S_2 when the anode side allows strong reduction conditions. Li_2S and Li_2S_2, which are generated via electrolysis of high-sulfur-content lithium polysulfide, are less soluble in the electrolyte. Thus, lithium polysulfide that is electrolyzed at the interphase of the anode accumulates on the surface of the anode during cycling. Li_2S and Li_2S_2 are insulators, so they interfere with anodic reactions, thereby plating and stripping the Li metal. The repeated depositions of Li_2S and Li_2S_2 induce capacity fading.[14]

There is another critical problem involved in the use of lithium metal as the negative electrode. Lithium is charged and discharged by the repeated stripping and plating actions; the uneven flow of lithium ions in these processes causes dendritic growth of lithium, which crosses the separator, and may cause serious problems by shorting the anode and cathode inside the cell. In addition, under strong reducing conditions of the anode, the electrolyte may decompose and react with lithium ions and electrons to form a solid–electrolyte interphase (SEI) layer. The SEI layer may be repeatedly formed on the lithium surface owing to the volume change of lithium during the charge and discharge processes; this forms dead lithium, causes low coulombic efficiency (C.E), and decreases the active material of the negative electrode. Many studies

have attempted to solve these cycling problems in batteries. Xiulei Ji et al. suggested using highly ordered carbon nanostructures to prevent the sulfur from dissolving into the electrolyte.[15] Weiyang Li et al. have shown that a stable and uniform SEI layer forms because of a synergetic effect of lithium polysulfide and lithium nitrate used as additives in an ether-based electrolyte, thereby preventing dendritic growths and minimizing electrolyte decomposition.[16] Yong-keon Ahn et al. showed through computer simulations (COMSOL) that anodic aluminum oxide (AAO) can evenly distribute the flux of lithium ions generated during charging and discharging on the surface of the lithium metal in order to effectively suppress the formation of lithium dendrites.[17]

1.2 Functional separator for lithium sulfur batteries

In this study, we propose a functional separator to solve two problems associated with LSBs using AAO and poly(vinylidene fluoride-co-hexafluoropropylene) (PVdF-HFP). The functional separator was made by filling PVdF-HFP on the surface of the AAO and inside the pores of the layer. AAO has highly ordered and a vertically formed nanopore structure, along with very stable electrochemical and thermal properties.[18] In addition, PVdF-HFP molecules swell within the electrolyte, which not only pass lithium ions well but also prevent lithium polysulfide from passing into the anode region.[19],[20] A PVdF-HFP coated AAO (PAAO) membrane was prepared by coating PVdF-HFP solution on AAO. The AAO provides a highly ordered vertical pore structure and has less tortuosity than a conventional separator. The vertical pore structure of the AAO evenly distributes the Li-ion flux in the battery system, so the proposed separator effectively prevents the non-uniform growth of lithium. The AAO is also mechanically, chemically, and thermally stable.[17] The vertically aligned pores of AAO are filled with PVdF-HFP to form a gel polymer electrolyte that offers high lithium-ion conductivity than conventional electrolytes. The PVdF-HFP selectively passes lithium ions and effectively blocks dissolution of the polysulfide into the anode region. Consequently, the

proposed scheme conserves high specific capacity with high C.E during cycling. The prepared PAAO showed high specific capacity (～850 mAh g^{-1}, 0.2C), high C.E (>98%), and long cycle life (75% retention @ 100 cycles, 0.5C). The reference polyethylene separator showed low specific capacity (～500 mAh g^{-1}, 0.2C), low C.E (~90%), and fast capacity fading (42% retention @ 100cycles, 0.5C) during cycling. Compared with a PP separator and bare AAO separator, the PAAO separator showed better initial capacity, C.E, and electrochemical stability. The suggested PAAO separator effectively blocks the polysulfide shuttle effect and improves the cyclability of the LSBs. This suggests that the proposed poreless separator may be a good candidate as a powerful separator for LSBs.

Chapter 2. Experimental Section

2.1 Fabrication of anodic aluminum oxide

The AAO membrane was fabricated by a two-step anodic oxidation method. First, a high-purity aluminum foil (99.999%, 500 μm, Goodfellow Ltd.) of appropriate size was prepared, its surface was washed with ethanol and acetone, and the foil was annealed at 500 °C to remove residual stress. Thereafter, to remove the natural oxide film on the aluminum surface by the electrochemical method, 20 V was applied via a polishing solution. The polishing solution was prepared by mixing ethanol and perchloric acid in the ratio of 4:1 (v:v) for about 8 min at a fixed temperature of 0 °C. After the surface of aluminum is cleaned through electrochemical polishing, the first anodization process commences. The anodizing process was conducted at 40 V and 15 °C in 0.3 M oxalic acid solution. After the first anodic oxidation, the aluminum oxide layer formed on the surface was removed by etching for 4 h in chromium(VI) oxide solution, and the second anodic oxidation was performed under the same conditions as the first process. Owing to the constant dimple produced on the aluminum surface by the first anodization, a more uniform pore structure could be obtained in the secondary anodization step. In addition, a pure aluminum substrate was obtained using a 1:1 solution of 0.3 M copper(II) chloride and hydrochloric acid. The bottom AAO barrier

layer was removed from the substrate by soaking in phosphoric acid solution for 60 min. The surface of this substrate was then observed using field emission-scanning electron microscope(FE-SEM) (Hitachi, S-4800) to understand the morphological and structural characteristics of the AAO.

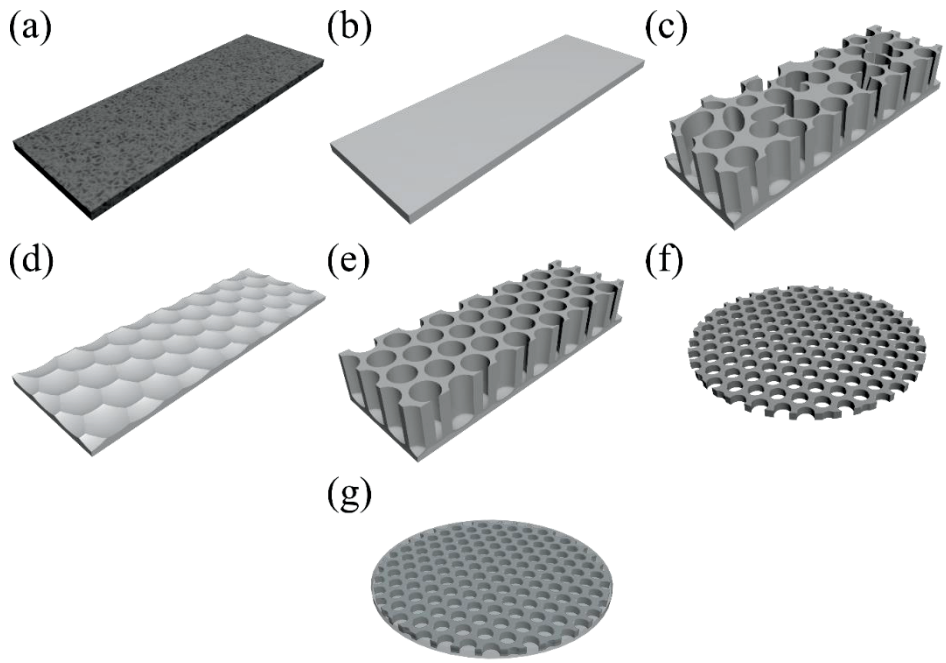

Figure 1. Fabrication process of AAO membrane: (a)aluminum foil, (b)aluminum after electrochemical polish, (c)after first anodization, (d)aluminum after remove first anodizing aluminum oxide layer, (e)after second anodization, (f)AAO membrane: after remove the barrier layer, (g)PAAO membrane: after coating with PVdF-HFP

2.2 Sulfur cathode

The sulfur electrode for the full cell test was prepared by slurry casting with a mixture of sulfur (Alfa Aesar), carbon black (Super P, Timcal), and polyethylene oxide (PEO, average Mv = 600,000, Sigma Aldrich) in a 6:2:2 mass ratio. The slurry was uniformly mixed using an orbital mixer (AR 100, Thinky mixer) and then cast in an aluminum foil using a doctor blade.

2.3 Electrochemical characterization

In order to evaluate the electrochemical properties of the fabricated membrane, several cells were assembled using the CR2032 coin cell and then evaluated. In the ion conductivity measurements, a 1 M LiTFSI in dimethyl ether (DME)/1,3-dioxolane (DOL) (volume ratio of 1/1) was used as the electrolyte and a stainless steel (SUS) coin cell can was used as the electrode. Ionic conductivity of the separators at room temperature was determined with two electrodes AC impedance method by using EC-Lab (VSP, Bio-Logic SAS) over a frequency range of 100 mHz to 1 MHz. After measuring the resistance by AC impedance, the ion conductivity was calculated using the following equation[21]:

$$ionic\ \ conductivity\ \ (\sigma) = \frac{L}{R_b A} \qquad \text{Eq. (1)}$$

where L is the thickness of the separator, R_b is the bulk resistance, and A is the contact area between the separator and SUS electrode.

All cycle tests were performed using an automated charge–discharge equipment (WBCS 3000L, WonATech).

Chapter 3. Results and Discussion

3.1 Structure analysis of anodic aluminum oxide

The morphological and physical characteristics of AAO and PAAO were confirmed via scanning electron microscopy (SEM). In Figure 1(a), it is seen that a highly ordered pore structure was formed on the surface of the AAO. The pore size is about 50 nm and the thickness is 25 μm (Figure 1). In Figure 1(b), we see that the barrier layer on the back of AAO substrate has been removed normally to form vertical pores. In the case of the PAAO, PVdf-HFP was dissolved in dimethylformamide (DMF) solution at 5 wt% and then rotated at 500 rpm for 30 s on the wafer to obtain a thin film. Then, before the DMF solution evaporated, the AAO was placed on the PVdf-HFP/DMF solution on the wafer to coat the surface of the AAO and absorb the PVdf-HFP inside the pores. The as-prepared PAAO has a thickness of 35 μm and is coated with PVdF-HFP on both the front and back sides, and as shown in the Figure 3, PVdF-HFP is well absorbed into the vertical pores.

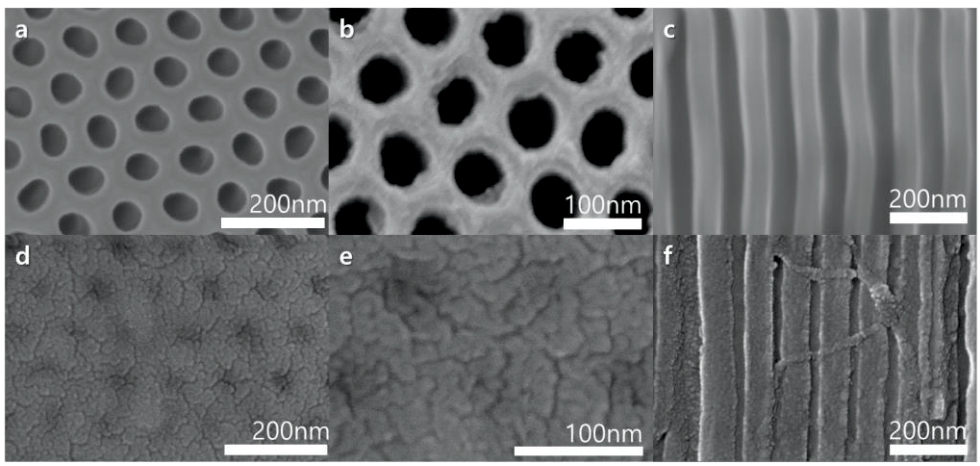

Figure 2. SEM characterization images of the AAO membrane and polymer coated AAO membrane: (a) front, (b) bottom, (c) cross-section of AAO membrane, and (d) front, (e) bottom, (f) cross-section of the polymer coated AAO membrane

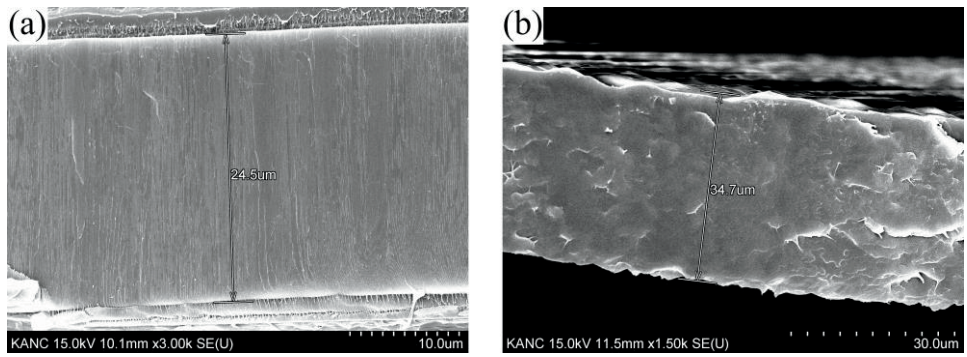

Figure 3. Thickness of the (a) AAO and (b) PAAO.

3.2 Separator characterization of PAAO

Among the many intrinsic properties of the membrane, there are a few critical ones, for example, the contact angle with the electrolyte, electrolyte uptake, porosity, wettability, and thermal stability. These characteristics directly affect the performance and stability when the separator is applied to a battery.[22],[23]

In order to evaluate the thermal stability of the prepared membrane, the shrinkage rate was evaluated after standing for 30 min at a temperature of 90 ℃ (Figure 4.) In the case of the AAO-containing separators such as PAAO or AAO, the membranes were thermally very stable and no shrinkage was observed at 90 ℃. However, shrinkage was observed at 90° in the PP membrane, and the thermal shrinkage was calculated from the following equation.[17]

$$\text{shrinkage}(\%) = \frac{(A_i - A_f)}{A_i} \qquad \text{Eq. (2)}$$

where A_i and A_f are the areas of the separator before and after the thermal stability test, respectively. The PP dimensional change is about 15% (Figure 4(a) and (d)). If the shape of the separator is changed by temperature, as in the case of the PP separator, there is the possibility that an internal short circuit may occur during the operation of the cell.

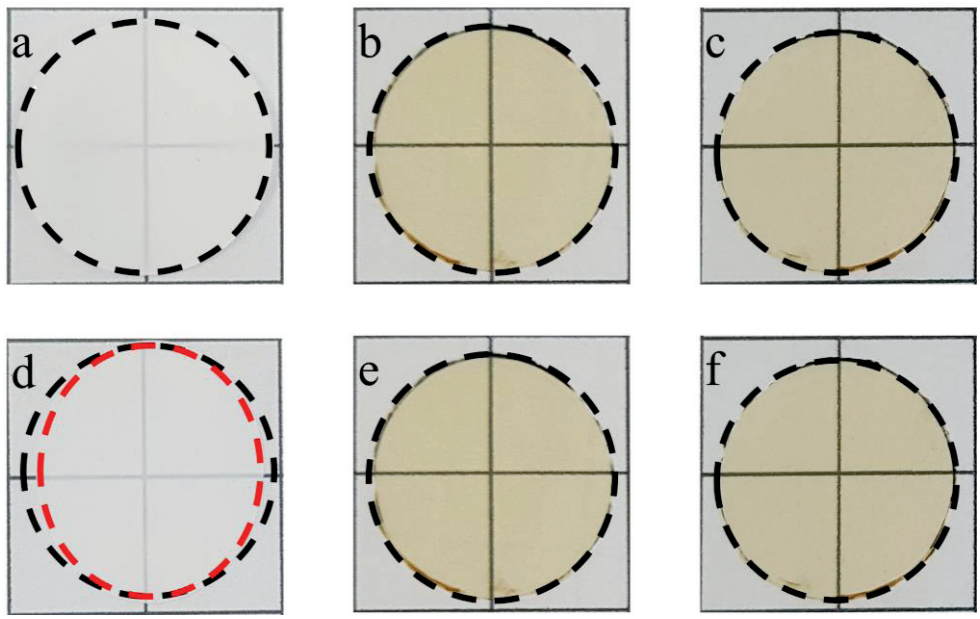

Figure 4. Before and after Thermal stability tests of PP (a and d), AAO (b and e) and polymer coated AAO (c and f)

Figure 5. Contact angle of the (a) PP, (b) Bare AAO, (c) polymer coated AAO

In figure 5, the contact angles of the membranes were measured to evaluate the affinity of the PAAO to shallow water. The electrolyte was measured using 1 M LiTFSI DME/DOL at a volume ratio of 1/1 (PANAX ETEC). The PP membrane was about 47°, and the AAO membrane was about 10°. The PAAO membrane was absorbed immediately after dropping, and the contact angle could not be measured. The AAO has a large number of micropores of approximate average size 50 nm, which can quickly absorb organic electrolytes owing to hydrophilicity, capillary force, and close polarity. The PAAO can also absorb electrolytes quickly by the swelling effect of the PVdF-HFP.[24]

$$Electrolyte\ uptake\ (\%) = \frac{W_w - W_d}{W_d} \times 100 \qquad \text{Eq. (3)}$$

Here, W_d and W_w are the weight of the dry separator and the weight of the separator sufficiently wetted with electrolyte, respectively. When comparing the electrolyte uptake, PP with 136%, AAO with 103%, and PAAO with 123% were observed. The PAAO showed lower electrolyte uptake than the PP membrane, but it could absorb more electrolyte than the AAO via the PVdF-HFP coating.

$$Porosity(\%) = \frac{W_f - W_i}{\rho_{liq} V_i} \times 100 \qquad \text{Eq. (4)}$$

where W_f is the weight of the membrane measured after soaking in n-butanol for 3 h, W_i is the weight of the pure membrane, ρ_{liq} is the density of n-butanol, and V_i is the volume of the membrane. From porosity

measurements, AAO 71.5%, and PAAO 67.2%. The porosity of the PP membrane was 55%.[25] These results indicate that AAO and PAAO have more porous structures than PP separators and can be completely wetted on the insides of the pores considering the organic electrolyte uptake measurements. This is due to the swelling effect of the PVdF-HFP; PVdF-HFP allows organic solvents to penetrate the spaces between the chains, thus absorbing more quantity of organic solvents.[26]

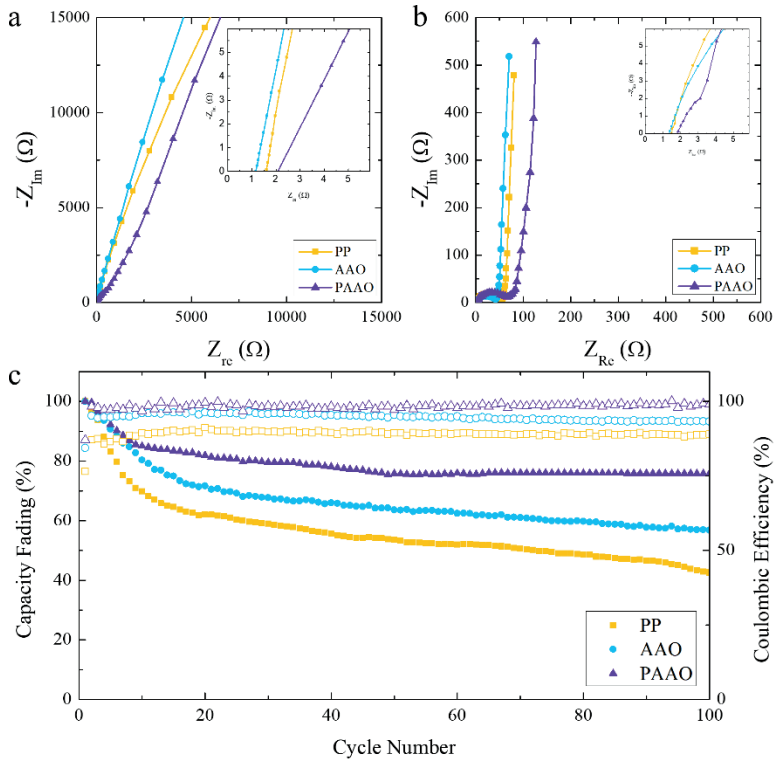

Figure 6. Electrochemistry performance of PP, AAO and PAAO. (a) ion conductivity measurement using ac impedance, (b) electrochemical impedance spectroscopy, (c) cycle performance.

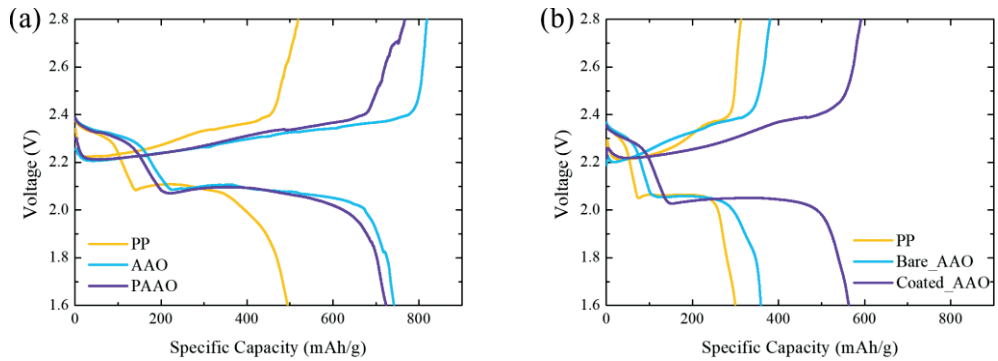

Figure 7. Voltage profile of lithium sulfur cell with each separat or at 0.5C. (a) first cycle, (b) 100th cycle

3.3 Electrochemical characterization of lithium sulfur cell

Through electrochemical analysis, the ion conductivity of the membrane and the impedance and charge/discharge characteristics when applied to the lithium sulfur cell were confirmed.[27],[28] The ionic conductivity of the metal/separator/metal structure was 0.55 mS cm^{-1} for PP, 1.52 mS cm^{-1} for AAO, and 1.01 mS cm^{-1} for PAAO (Figure 6(a)). The PAAO showed higher ionic conductivity than commercial membranes owing to the structural properties of the AAO. The highly ordered vertical pores in AAO increase the ion conductivity by providing a passage through which lithium ions move, hence providing a straighter path than commercial polyolefin separators. When the bulk resistance was measured through AC impedance in a full cell using lithium metal as a negative electrode and sulfur as a positive electrode active material, PP showed 1.48 Ω, AAO showed 1.36 Ω, and PAAO showed 1.77 Ω (Figure 6(b)). AAO showed lower resistance than PP as well as PAAO. In addition, the charge transfer conductivity was measured as 21.3×10^{-3} mS cm^{-1} for PP, 35.8×10^{-3} mS cm^{-1} for AAO, and 25.1×10^{-3} mS cm^{-1} for PAAO. Owing to the structural characteristics of AAO, the AAO is superior to PP in all measurements; however, PAAO is superior to PP and slightly lower than AAO. This result indicates that the thickness of the PAAO increased during the

PVdF-HFP coating process, and therefore, the performance faded. When 100 cycles were charged and discharged at 0.5C in a full cell, both PP and AAO maintained only 55% of their capacity after 100 cycles. On the other hand, when PAAO was applied, the capacity was maintained at 75%, and the C.E was over 98%. In particular, there is a marked difference in the second plateau section at 2–2.1 V. In Figure 7 (a) and (b), after 100 cycles, only the PAAO-applied cell was sustained in the second plateau, and the remaining PP and AAO were very short. In the second plateau, the following reactions occur:[29],[30]

$$Li_2S_4 + \ 2e^- + \ 2Li^+ \ \rightarrow \ 2Li_2S_2 \qquad \text{Eq. (5)}$$

$$2Li_2S_2 + 4e^- + 4Li^+ \ \rightarrow 4Li_2S \qquad \text{Eq. (6)}$$

At this time, as the length of the lithium polysulfide becomes shorter, a large amount of lithium is precipitated on the surface of the lithium metal beyond the separator, and the amount of remaining active material decreases, thereby gradually decreasing the capacity. Therefore, it can be seen that the PAAO effectively blocks the lithium polysulfide species. This is possible because PVDF-HFP, which is located on the surface and inside the pores of the AAO, effectively blocks lithium polysulfide and only passes lithium ions.

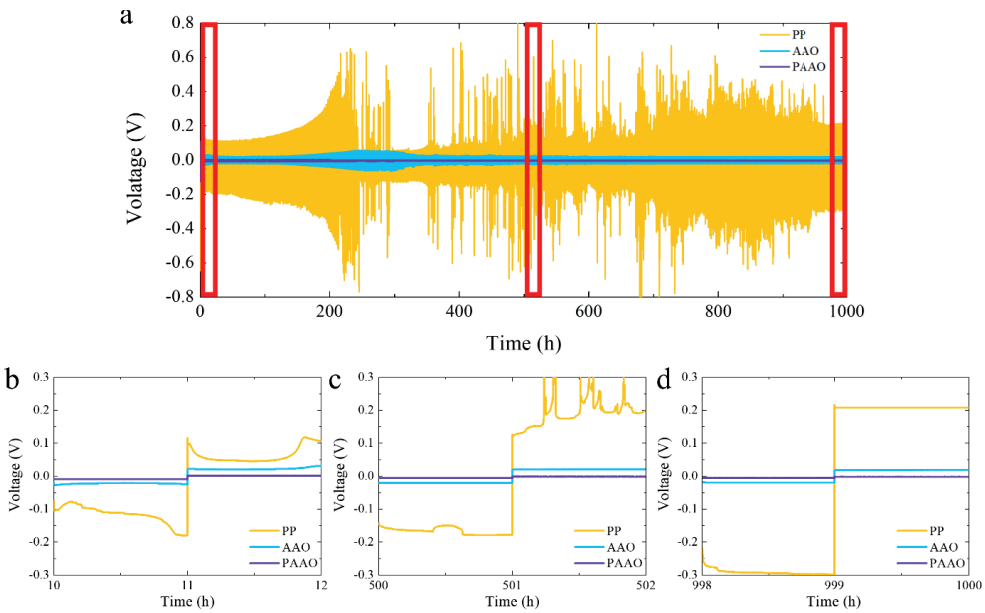

Figure 8. The voltage profile of Li symmetric cell cycled galvanostatically at 1 mA cm^{-2} for 500 cycles.

In Figure 8, the stability of the lithium interface during charging and discharging was investigated through the lithium symmetric cell. The experiment was conducted under the conditions of 1 mA cm^{-2} and 1 mAh cm^{-2}. Figure 8(b) shows the voltage profile during the initial cycle and shows two peaks at each plating and stripping stage. This phenomenon occurs because the kinetic pathway is different between the interface of the lithium metal electrode and the electrolyte; this phenomenon is also apparent at the beginning of the cycle and gradually disappears as the cycle progresses.[31] In PAAO, however, the voltage behavior of the double peak shape is not observed. Only the plateau shape appears. In the case of PP separators, the lithium plating and stripping cycles are repeated, resulting in thick inactive layers due to lithium build-up on the surface of the lithium electrode and increasing over potential. Therefore, lithium ions are prevented from continuously accumulating and growing in only one portion, thereby preventing dendrite formation and enabling long-term charge and discharge. Therefore, it can be seen that the PAAO separator can greatly improve the unstable charge/discharge characteristics of the lithium metal.[32]

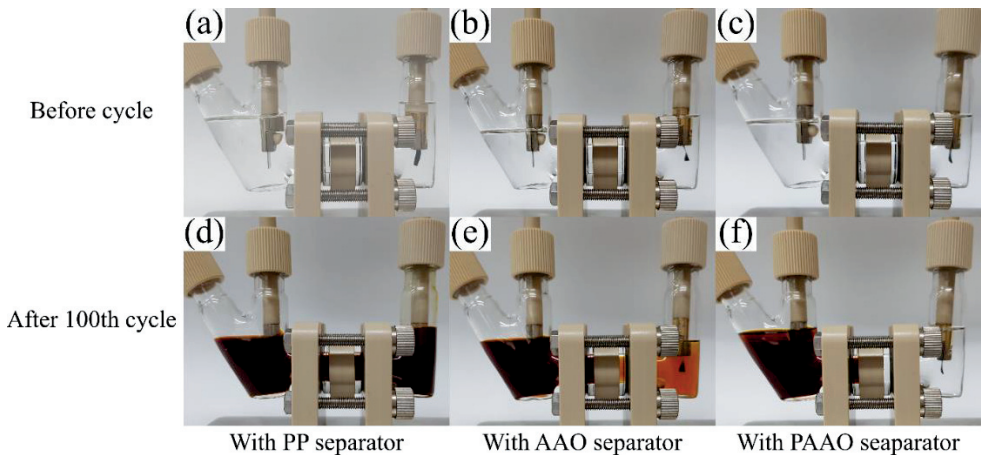

Figure 9. Optical Image of dissolution and diffusion of poly sulf ide during the charge-discharge process.

In Figure 9, we observed the movement of lithium polysulfide during charging and discharging using H-cell in real time.[33] When the PP separator is applied, it can be seen that all of the poly sulfide has passed to the anode region in 100 cycles. On the other hand, in the case of AAO and PAAO, it can be seen that it effectively limited polysulfide movement. PAAO limited the movement of polysulfide via the PVdF-HFP located on the AAO. In the case of AAO, the strong interaction between polysulfide and AAO seems to limit some polysulfide movement.[34]

Chapter 4. Conclusion

In this study, we present a functional separator (PAAO) that can be applied to LSBs via a composite of organic and inorganic materials. PAAO effectively prevents the continuous reduction of capacity due to the shuttle effect of lithium polysulfide, which is the biggest problem of LSBs. In addition, by utilizing the structural advantages of AAO, which is an inorganic material, the flux of lithium ions is effectively distributed, and the surface of the lithium metal anode is stably controlled, thereby increasing the utility of the lithium metal as a cathode. Therefore, this concept can easily solve the problem of continuous capacity reduction due to the shuttle effect of polysulfide in LSBs, and the stability problem of lithium metal with one separator.

References

1. Tarascon, J.-M. & Armand, M. Issues and challenges facing rechargeable lithium batteries. *Nature* **414**, 359–367 (2001).
2. Dunn, B., Kamath, H. & Tarascon, J.-M. Electrical Energy Storage for the Grid: A Battery of Choices. *Science.* **334**, 928–935 (2011).
3. Bruce, P. G., Freunberger, S. A., Hardwick, L. J. & Tarascon, J.-M. Li–O_2 and Li–S batteries with high energy storage. *Nat. Mater.* **11**, 19–29 (2012).
4. Lu, L., Han, X., Li, J., Hua, J. & Ouyang, M. A review on the key issues for lithium-ion battery management in electric vehicles. *J. Power Sources* **226**, 272–288 (2013).
5. Goodenough, J. B. & Park, K.-S. The Li-Ion Rechargeable Battery: A Perspective. *J. Am. Chem. Soc.* **135**, 1167–1176 (2013).
6. Nitta, N., Wu, F., Lee, J. T. & Yushin, G. Li-ion battery materials: present and future. *Mater. Today* **18**, 252–264 (2015).
7. Whittingham, M. S. Lithium Batteries and Cathode Materials. *Chem. Rev.* **104**, 4271–4302 (2004).
8. Manthiram, A., Fu, Y., Chung, S.-H., Zu, C. & Su, Y.-S. Rechargeable Lithium–Sulfur Batteries. *Chem. Rev.* **114**, 11751–11787 (2014).
9. Xu, W. *et al.* Lithium metal anodes for rechargeable batteries. *Energy Environ. Sci.* **7**, 513–537 (2014).
10. Yang, H. *et al.* Recent progress and perspective on lithium metal anode protection. *Energy Storage Mater.* **14**, 199–221 (2018).

11. Fang, C., Wang, X. & Meng, Y. S. Key Issues Hindering a Practical Lithium-Metal Anode. *Trends Chem.* **1**, 152–158 (2019).

12. Mikhaylik, Y. V. & Akridge, J. R. Polysulfide Shuttle Study in the Li/S Battery System. *J. Electrochem. Soc.* **151**, A1969 (2004).

13. Barchasz, C. *et al.* Lithium/Sulfur Cell Discharge Mechanism: An Original Approach for Intermediate Species Identification. *Anal. Chem.* **84**, 3973–3980 (2012).

14. Deng, Z. *et al.* Electrochemical Impedance Spectroscopy Study of a Lithium/Sulfur Battery: Modeling and Analysis of Capacity Fading. *J. Electrochem. Soc.* **160**, A553–A558 (2013).

15. Ji, X., Lee, K. T. & Nazar, L. F. A highly ordered nanostructured carbon–sulphur cathode for lithium–sulphur batteries. *Nat. Mater.* **8**, 500–506 (2009).

16. Li, W. *et al.* The synergetic effect of lithium polysulfide and lithium nitrate to prevent lithium dendrite growth. *Nat. Commun.* **6**, 7436 (2015).

17. Ahn, Y. *et al.* Enhanced electrochemical capabilities of lithium ion batteries by structurally ideal AAO separator. *J. Mater. Chem. A* **3**, 10715–10719 (2015).

18. Lee, W. & Park, S.-J. Porous Anodic Aluminum Oxide: Anodization and Templated Synthesis of Functional Nanostructures. *Chem. Rev.* **114**, 7487–7556 (2014).

19. Shin, J. H., Jung, S. S., Kim, K. W., Ahn, H. J. & Ahn, J. H. Preparation

and characterization of plasticized polymer electrolytes based on the PVdF-HFP copolymer for lithium/sulfur battery. *J. Mater. Sci. Mater. Electron.* **13**, 727–733 (2002).

20. Shalu, S., Singh, V. K. & Singh, R. K. Development of ion conducting polymer gel electrolyte membranes based on polymer PVdF-HFP, BMIMTFSI ionic liquid and the Li-salt with improved electrical, thermal and structural properties. *J. Mater. Chem. C* **3**, 7305–7318 (2015).

21. Xu, W. Ionic Conductivity and Electrochemical Characterization of Novel Microporous Composite Polymer Electrolytes. *J. Electrochem. Soc.* **146**, 4410–4418 (1999).

22. Arora, P. & Zhang, Z. (John). Battery Separators. *Chem. Rev.* **104**, 4419–4462 (2004).

23. Yao, H. *et al.* Improved lithium–sulfur batteries with a conductive coating on the separator to prevent the accumulation of inactive S-related species at the cathode–separator interface. *Energy Environ. Sci.* **7**, 3381–3390 (2014).

24. Wang, H. *et al.* Pyrogallic acid coated polypropylene membranes as separators for lithium-ion batteries. *J. Mater. Chem. A* **3**, 20535–20540 (2015).

25. Xu, Q. *et al.* Polydopamine-coated cellulose microfibrillated membrane as high performance lithium-ion battery separator. *RSC Adv.* **4**, 7845 (2014).

26. Suthar, B., Northrop, P. W. C., Rife, D. & Subramanian, V. R. Effect of Porosity, Thickness and Tortuosity on Capacity Fade of Anode. *J.*

Electrochem. Soc. **162**, A1708–A1717 (2015).

27. Wong, D. H. C. *et al.* Phase Behavior and Electrochemical Characterization of Blends of Perfluoropolyether, Poly(ethylene glycol), and a Lithium Salt. *Chem. Mater.* **27**, 597–603 (2015).

28. Zahn, R., Lagadec, M. F., Hess, M. & Wood, V. Improving Ionic Conductivity and Lithium-Ion Transference Number in Lithium-Ion Battery Separators. *ACS Appl. Mater. Interfaces* **8**, 32637–32642 (2016).

29. Shen, C. *et al.* Understanding the role of lithium polysulfide solubility in limiting lithium-sulfur cell capacity. *Electrochim. Acta* **248**, 90–97 (2017).

30. Liu, Q. *et al.* Insight on lithium polysulfide intermediates in a Li/S battery by density functional theory. *RSC Adv.* **7**, 33373–33377 (2017).

31. Chen, K.-H. *et al.* Dead lithium: mass transport effects on voltage, capacity, and failure of lithium metal anodes. *J. Mater. Chem. A* **5**, 11671–11681 (2017).

32. Wood, K. N. *et al.* Dendrites and Pits: Untangling the Complex Behavior of Lithium Metal Anodes through Operando Video Microscopy. *ACS Cent. Sci.* **2**, 790–801 (2016).

33. Song, H. *et al.* A thin TiO_2 NTs/GO hybrid membrane applied as an interlayer for lithium–sulfur batteries. *RSC Adv.* **8**, 429–434 (2018).

34. Qu, H. *et al.* Inorganic separators enable significantly suppressed polysulfide shuttling in high-performance lithium–sulfur batteries. *J. Mater. Chem. A* **6**, 23720–23729 (2018).

요 약 (국문 초록)

리튬 황-전지에서의 폴리설파이드의 셔틀 효과를 막는 기능성 분리막

조진일

융합과학부 나노융합전공

서울대학교 대학원

리튬 이온 배터리 (LIB)는 높은 에너지 밀도, 재충전 특성 및 작은 메모리 효과로 인해 휴대용 전자 장치에 널리 사용되어왔다. 그러나 첨단 휴대용 전자 장치, 전기 자동차 (EV) 및 대규모 에너지 저장 시스템 (ESS)은 높은 에너지 밀도, 경량 및 저비용 LIB를 필요로 한다.

황은 지구상에서 가장 풍부한 물질 중 하나이며 이론적 인 용량이 높다. 그러나 몇 가지 문제가 있다. 첫 번째 문제는 폴리 설파이드의 용해이다. 충전 및 방전 과정 동안 형성되는 리튬 폴리 설파이드는 LIB의 유기 전해질에 가용성이다. 이는 연속적인 양극 활물질 소비로 이어지고, 결국 용량은 사이클이 반복되면서 줄어든다. 두 번째 문제는 양극으로 사용되는 리튬 금속의 안전성과 안정성입니다. 리튬 금속 표면 제어는 Li 금속 음극의 안정성 뿐만 아니라 높은 쿨롱 효율과 고 용량을 위해 필요한 단계이다.

본 연구에서 우리는 polysulfide 셔틀 효과를 방지하고 리튬 금속 계면을 제어하기 위해 poly (vinylidene fluoride-co-hexafluoropropene) (PVdF-HFP)로 코팅 된 양극 산화 알루미늄 (PAAO) 분리막을 개발하였다. 양극 산화 알루미늄 (AAO) 상에 PVdF-HFP 용액을 코팅하여 PAAO를 제조 하였으며 AAO는 기계적, 화학적 및 열적 안정성을 제공한다. AAO의 수직 정렬 기공은 겔 폴리머 전해질로 사용 된 PVdF-HFP로 채워지며, 기존의 전해질과 함께 높은 리튬 이온 전도성을 제공한다. PVdF-HFP는 리튬 이온을 선택적으로 통과시키고 폴

리 설파이드가 음극영역으로의 용해를 효과적으로 차단한다. 결과적으로, 제안된 시스템은 사이클 동안 높은 쿨롱 효율로 높은 용량을 유지했다. 제조 된 PAAO는 높은 비 용량 (~ 850 mAh / g, 0.2C), 높은 쿨롱 효율 (> 98 %) 및 긴 사이클 수명 (> 100 사이클, 0.5C)을 나타냈다. 제안 된 PAAO 분리기는 폴리 설파이드 셔틀 효과를 효과적으로 차단하고 LI-S 시스템의 열악한 사이클 특성을 개선할 수 있다.

주요어 : 리튬-황 전지, 리튬 금속, 고분자 전해질, 양극산화 알루미늄 차세대 배터리

학 번 : 2018-21383